



A New Corrosion Inhibitor for Mild Steel: Experimental and Theoretical Studies

Ekerete Jackson^{1,*}, K. E. Essien² and P. C. Okafor³

¹Department of Chemistry, Faculty of Science, University of Uyo, P.M.B 1017, Uyo, AkwaIbom State, Nigeria.

²Department of Science Technology, AkwaIbom State Polytechnic, IkotOsurua, P. M. B. 1200, AkwaIbom State, Nigeria.

³Department of Pure and Applied Chemistry, University of Calabar, P.M.B 1115, Calabar, Nigeria.

ARTICLE INFO

Article history:

Received: 28 May 2015;

Received in revised form:

20 August 2015;

Accepted: 8 September 2015;

Keywords

D - Tryptophan (DT),
Temkin adsorption isotherm,
Electrochemical impedance
Spectroscopy,
Potentiodynamic polarization,
Corrosion inhibition,
Mild steel (MS).

ABSTRACT

The corrosion inhibition and adsorption process of D - Tryptophan (DT) on mild steel in 2 HCl was studied by means of chemical (weight loss), electrochemical and quantum chemical techniques. The inhibition efficiency increases with decreasing temperature and increasing concentration of inhibitor. It has been determined that the adsorption of DT on mild steel obeys the Temkin adsorption isotherm at all studied temperatures with negative values of ΔG_{ads}^0 , suggesting a stable and a spontaneous inhibition process. In potentiodynamic polarization, the curves shifted towards lower current density in the presence of the DT with well-defined Tafel regions suggesting that the inhibitor retard the corrosion process without changing the mechanism of the corrosion process; and exhibit cathodic and anodic polarization (mixed type inhibitor) because the change in E_{corr} is less than 85 mV/SCE with respect to the blank. Corrosion current density was calculated by extrapolation of the linear parts of these curves to the corresponding corrosion potential; and corrosion potential (E_{corr}), corrosion current densities (i_{corr}), anodic Tafel slope (β_a), cathodic Tafel slope (β_c) were determined with maximum value of inhibition efficiency for 5×10^{-4} M concentration of the inhibitor at 303 K was 78.4%. From Nyquist plot of electrochemical impedance spectroscopy, values of polarization resistance (R_p) increased with increasing inhibitor concentration whereas double layer capacitance (C_{dl}) decreased indicating a decrease in local dielectric constant or an increase in thickness of electric double layer suggesting that the inhibitor function by forming a protective layer at the metal surface. Quantum chemical calculations were performed using Density Functional Theory (DFT) with the help of complete geometry optimization for theoretical calculations of E_{HOMO} , E_{LUMO} , and energy gap (ΔE). Inhibition efficiency increases with increasing E_{HOMO} indicating that the molecule has tendency to donate electrons to the mild steel with low energy empty molecular orbital; whereas low value of E_{LUMO} suggests that the molecule easily accepts electrons from mild steel.

© 2015 Elixir All rights reserved.

Introduction

Organic inhibitors are commonly used in acid solutions to reduce the corrosive attack to the contacted metallic materials, among which steel is extensively used [1-3]. Acid pickling, Industrial cleaning, acid descaling, oil-well acidizing in oil recovery and the petrochemical processes are the most important fields of applications of acid solutions. One of the most corrosive media is the aqueous solutions of acids. Hence, the rate of corrosion at which metals are destroyed in acidic media is very high, especially when soluble corrosion products are formed. Hence, investigating and exploring corrosion inhibitors for steel corrosion in acid solutions are important for both academic point of view and also for its practical applications [4-5]. Researchers have shown that most of the efficient organic inhibitors containing nitrogen, oxygen, sulphur, double and triple bonds have some lone pair of electrons and π bonds existing in their molecules which serve as adsorption sites [6]. The acid inhibitors are adsorbed on the metal surface thereby blocking the active sites on the surface hence reducing the corrosion rate.

However, there is no literature to date about the corrosion inhibitive effect of D-tryptophan (DT) on mild steel in HCl solution. Hence, this work deals with the study of the corrosion inhibition properties of D-tryptophan. The aim of this study was to determine the inhibition efficiency of DT as an inhibitor for the corrosion of mild steel in 2 M HCl. The choice of this compound was also based on molecular structure considerations, i.e. this is an organic compound with several adsorption centres. The molecular structure of D - Tryptophan (DT) is given in Fig 1. Three techniques were employed to carry out the measurements: (a) chemical (weight loss) (b) electrochemical (potentiodynamic polarization) and (c) molecular modeling.

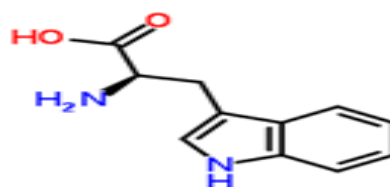


Fig 1. The chemical structure of D - Tryptophan (DT)

Tele:

E-mail addresses: ekeretejackson@yahoo.com

© 2015 Elixir All rights reserved

Experimental Method

Materials

Material used for the study was mild steel sheet. The sheet was mechanically pressed cut into coupons of dimensions 5 x 4 x 0.11 cm for weight loss studies and 2 x 1.5 x 0.11 cm for electrochemical studies with a hole made for insertion of the hooks. The coupons were polished with series of emery paper of variable grades starting with the coarsest and then proceeding in steps to the finest (600) grade, degreased with ethanol, dipped in acetone and allowed to dry in the air before it was preserved in a desiccator [6,7,8,9]. All reagents used for the study were Analar grade and distilled water was used for their preparation. The chemical composition of the mild steel used is as shown in Table 1.

Gravimetric measurements

The apparatus and procedure followed for the weight loss measurements were as previously reported [10 -15]. The corroding concentration was kept at 2 M HCl and the volume of the test solution used was 100 mL. All tests were made in aerated solutions. The difference between the weight at a given time and the initial weight of the coupons was taken as the weight loss which was used to compute the corrosion rate given by [16]:

$$\text{Corrosion rate, } \rho = \frac{\Delta W}{A t} \quad (1)$$

Where, ΔW is the weight loss, A is the total area of the mild steel coupon, t is the corrosion time and ρ is the corrosion rate.

$$\text{Surface Coverage, } \theta = \frac{\rho_1 - \rho_2}{\rho_1} \quad (2)$$

$$\text{Inhibition efficiency, } \% I = \frac{\rho_1 - \rho_2}{\rho_1} \times 100 \quad (3)$$

Where, ρ_1 and ρ_2 are the corrosion rates of the mild steel in 2 M HCl (blank) in the absence and presence of inhibitor respectively.

Polarization measurement

The working electrode was immersed in test solution for 30 minutes until a steady state open circuit potential (E_{ocp}) was obtained. The polarization curve was recorded under potentiodynamic polarization conditions and under air atmosphere and it was controlled by a personal computer. After the open circuit potential had been established, dynamic polarization curves were obtained at a scan rate of 1 mV/s in the potential range from - 0.25 V to 0.25 V. Corrosion current density (i_{corr}) values were obtained by the Tafel extrapolation method. All potentials were measured against SCE. The percentage inhibition efficiency (η), was calculated using the equation [17]

$$\eta(\%) = \frac{i_{corr}^0 - i_{corr}}{i_{corr}^0} \times 100 \quad (4)$$

Where, i_{corr}^0 and i_{corr} are values of corrosion current density in the absence and presence of inhibitor respectively.

Electrochemical impedance spectroscopy measurement

The electrochemical impedance spectroscopy measurements were carried out over a frequency domain from 10 Hz to 100,000 Hz at 303 K using amplitude of 5 mV RMS peak to peak with an ac signal at the open circuit potential and an air atmosphere. The impedance data were obtained using Nyquist plots and the polarization resistance R_p was obtained from the diameter of the semicircle in Nyquist plot. The polarization resistance (R_p) includes charge transfer resistance (R_{ct}), diffuse layer resistance (R_d), the resistance of accumulated species at the metal/solution interface (R_a) and the resistance of the film (in the presence of the inhibitor) at the metal surface (R_f). The percentage inhibition efficiency (η) was calculated from the

polarization resistance values obtained from the impedance measurements according to the relation [17]

$$\eta(\%) = \frac{R_p(inh) - R_p}{R_p(inh)} \times 100 \quad (5)$$

where $R_p(inh)$ and R_p are the charge transfer resistance in the presence and absence of inhibitor respectively. The double layer capacitance (C_{dl}) was calculated using the equation

$$C_{dl} = \frac{1}{2\pi f_{max} R_p} \quad (6)$$

where f_{max} is the frequency at the maximum in the Nyquist plot.

Computational details

First principle calculations were carried out using density functional theory (DFT) under the generalized gradient approximation (GGA) with Perdew – Burke – Ernzerhof (PBE) exchange correlation functional as implemented in Dmol³ module using material studio software package version 6.0. The quantum chemical indices considered were: the energy of the highest occupied molecular orbital (E_{HOMO}), the energy of the lowest unoccupied molecular orbital (E_{LUMO}), Energy gap = $E_{HOMO} - E_{LUMO}$, total energy, and Mulliken charges [18].

Results and Discussion

Experimental results

The corrosion inhibition efficiency (% IE), corrosion rate (CR) and surface coverage (θ) of D-typtophan (DT) after 10 hours of immersion at different temperatures (303 to 333K) are presented in Table 2. It is observed that the inhibition efficiency increased with increasing concentration of the inhibitor. In the absence of any inhibitor, the corrosion rate of mild steel increased steeply with increase in temperature. The corrosion rate was much lower in the presence of inhibitors than in the absence of any inhibitor at any temperature resulting in the retardation of the rate at which the metal goes into solution.

The adsorption characteristics of the inhibitor (DT) were investigated by fitting data obtained for the degree of surface coverage in different adsorption isotherms including Langmuir, Temkin, Freundlich, Florry-Huggins, Frumkin and Bockris-Swinkel adsorption isotherms. The test indicated that the adsorption was best described by Temkin adsorption model which is expressed as follows:

$$\exp(f\theta) = K_{ads} C \quad (7)$$

Where, K_{ads} is the equilibrium constant of the adsorption process, C is the inhibitor concentration, θ is the surface coverage, and f is the factor of energetic inhomogeneity of the metal surface describing the molecular interactions in the adsorption layer.

Fig. 2 is a plot of surface coverage against logarithm of inhibitor concentration. The correlation coefficient (R^2) was in the range 0.950 to 0.988 for all the inhibitors which is close to unity, indicating that the adsorption of the inhibitors is consistent with Temkin adsorption model.

The parameter f is defined as follows:

$$f = -2a \quad (8)$$

Where, a is molecular interaction parameter. The calculated values of a and equilibrium constant of the adsorption process (K_{ads}) obtained from Temkin adsorption plots are shown in table 3.

$$\exp(-2a\theta) = K_{ads} C \quad (9)$$

Eq. 8 clearly shows that the sign between f and a is reverse; that is, if $a < 0$, $f > 0$ and if $a > 0$, $f < 0$. Accordingly, if $f > 0$, mutual repulsion of molecules occurs, but if $f < 0$ attraction occurs [19]. Where, K_{ads} denotes the strength between adsorbate and adsorbent. Large values of K_{ads} indicate more efficient adsorption and hence better inhibition efficiency. From table 3, values of K_{ads} are very low indicating weak interaction between

the inhibitor and the mild steel surface. The equilibrium constant of adsorption K_{ads} is related to the standard free energy of adsorption (ΔG_{ads}^0), with the following equation [19].

$$K_{ads} = \frac{1}{55.5} \exp\left(\frac{\Delta G_{ads}^0}{RT}\right) \quad (10)$$

Where, R is the molar gas constant, T is temperature and 55.5 is concentration of water in solution expressed in molar. Rearranging the Equation (10) gives

$$\log K_{ads} = 1.744 - \frac{\Delta G_{ads}^0}{2.303RT} \quad (11)$$

Hence, the standard free energy of adsorption (ΔG_{ads}^0) was calculated from the above equation (11) and presented in table 3. Generally, values of ΔG_{ads}^0 around -20 kJmol^{-1} are consistent with electrostatic interactions between the charged molecules and the metal (Physisorption) while those around -40 kJmol^{-1} or higher are associated with chemisorption as a result of sharing or transfer of electrons from organic molecules to the metal surface to form a coordinate type of bond (chemisorption). One can see from Table 3 that the calculated ΔG_{ads}^0 values are around -20 kJmol^{-1} , indicating, therefore that the adsorption mechanism of the DT on the mild steel in 2 M HCl solution was typical of physisorption. Therefore, the adsorption of the studied DT on a mild steel surface is spontaneous and is consistent with the mechanism of electrostatic transfer of charge from the charged inhibitor molecule to the charged metal surface.

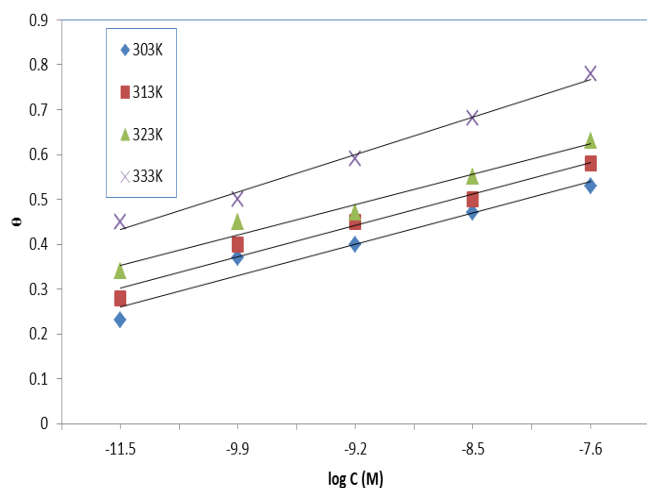


Fig 2. Temkin isotherm for the adsorption of DT on mild steel surface

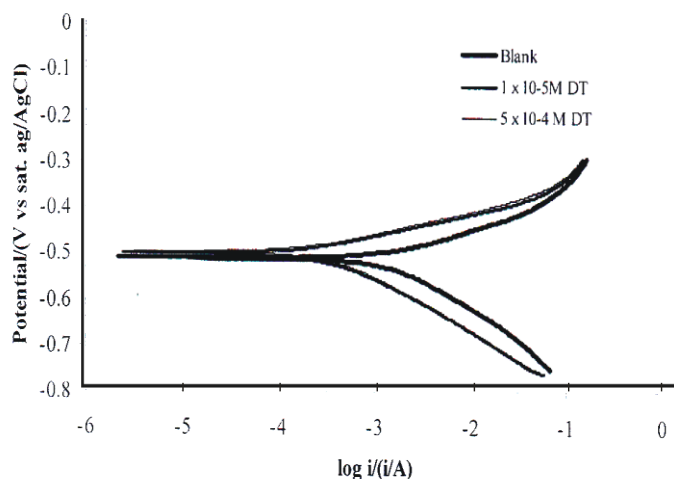


Fig 3. Potentiodynamic polarization curve for mild steel in 2 M HCl in the presence and absence of DT at 30°C

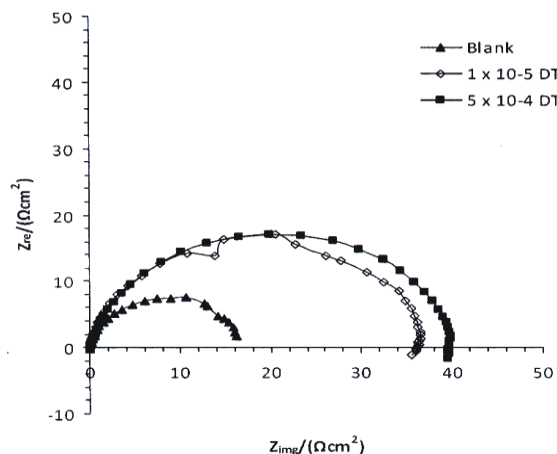


Fig 4. Nyquist plot for the corrosion of mild steel in 2 M HCl solution in the absence and presence of DT at 30°C

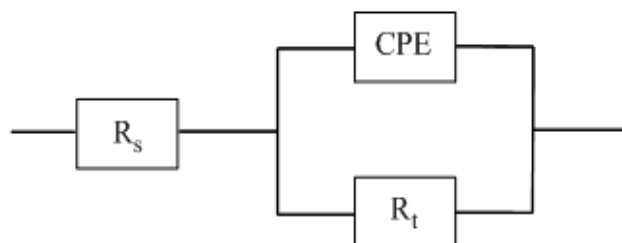


Fig. 5. Equivalent circuit for MS in 2 M HCl solution.

Electrochemical Impedance Study (EIS)

The electrochemical impedance data are depicted as Nyquist plot in Fig. 4. Analysis of the Nyquist plot (Fig. 4) showed a depressed capacitance loop which arises from the time constant of the electrical double layer and charge transfer resistance. The deviation of semicircles from perfect circular shape is often referred to the frequency dispersion of interfacial impedance [20]. This behavior is usually attributed to the inhomogeneity of the metal surface arising from surface roughness or interfacial phenomena [21], which is typical for solid metal electrodes [22]. The polarization resistance R_p was obtained from the diameter of the semicircle in Nyquist plot. The polarization resistance (R_p) includes charge transfer resistance (R_{ct}), diffuse layer resistance (R_d), the resistance of accumulated species at the metal/solution interface (R_a) and the resistance of the film (in the presence of the inhibitor) at the metal surface (R_f). From the values of polarization resistance (R_p) and double layer capacitance (C_{dl}) obtained from Nyquist plots and the calculated inhibition efficiency value (η %), it is obvious that the value of R_p increased with increasing concentration of inhibitor. The increase in R_p values is attributed to the formation of an insulating protective film at the metal/solution interface. It is also obvious that the value of C_{dl} decreased upon the addition of each of the inhibitor concentration indicating a decrease in the local dielectric constant and/or an increase in the thickness of the electric double layer suggesting that the inhibitors functioned by forming a protective layer at the metal surface. Generally, when a non-ideal frequency response is present, it is commonly accepted to employ the distributed circuit elements in the equivalent circuits. What most widely used is the constant phase element (CPE), which has a non-integer power dependence on the frequency [23, 24].

Table 1. Chemical Composition of Mild Steel Samples (Wt %)

C	0.17
Si	0.26
Mn	0.46
P	0.0047
S	0.017
Fe	Bal.

Table 2. Calculated Values Of Corrosion Rate Of Mild Steel (Cr), Degree Of Surface Coverage (Θ) And Inhibition Efficiency (% IE) Of Dt At 303 To 333k

Inhibitor	Conc. $\times 10^{-4}$ (M)	303 K			313 K			323 K			333 K		
		CR $\text{gcm}^{-2}\text{m}^{-1}$ $\times 10^{-4}$	Θ	% IE	CR $\text{gcm}^{-2}\text{m}^{-1}$ $\times 10^{-4}$	Θ	% IE	CR $\text{gcm}^{-2}\text{m}^{-1}$ $\times 10^{-4}$	Θ	% IE	CR $\text{gcm}^{-2}\text{m}^{-1}$ $\times 10^{-4}$	Θ	% IE
DT	Blank	8.55	-	-	12.75	-	-	19.60	-	-	29.60	-	-
	5.0	4.05	0.53	53	5.35	0.58	58	7.30	0.63	63	6.55	0.78	78
	2.0	4.50	0.47	47	6.38	0.50	50	8.85	0.55	55	9.50	0.68	68
	1.0	5.10	0.40	40	7.01	0.45	45	10.40	0.47	47	12.15	0.59	59
	0.5	5.35	0.37	37	7.65	0.40	40	10.78	0.45	45	14.80	0.50	50
	0.1	6.58	0.23	23	9.20	0.28	28	12.90	0.34	34	16.30	0.45	45

Table 3. Temkin parameters for the adsorption of DT on mild steel surface at 303 - 333 K

Inhibitor	T (K)	Intercept	Slope	K (mol/L)	f	a	$-\Delta G$ (kJ/mol)	R^2
DT	303	0.190	0.070	15.03	14.283	-7.142	16.945	0.950
	313	0.232	0.070	27.39	14.288	-7.142	19.066	0.971
	323	0.284	0.068	65.37	14.706	-7.353	22.011	0.970
	333	0.348	0.084	62.80	11.905	-5.953	22.581	0.988

Table 4. Electrochemical Parameters And Inhibition Efficiency (H%) Obtained From Polarization Studies Of Mild Steel In 2 M Hcl Solution In The Presence And Absence Of Dt At 303 K

Inhibitor	Concentration M $\times 10^{-4}$	E _{corr} V _m	I _{corr} $\mu\text{A cm}^2$	B _c m V dec ⁻¹	B _a $\mu\text{A m V dec}^{-1}$	$\eta\%$
Blank		-510	1563	157	103	
DT	0.1	-499	363	118	59	69.7
	5.0	-495	338	114	67	78.4

Table 5. Electrochemical Impedance Spectroscopy Parameters And Inhibition Efficiency (H %) For Mild Steel In 2 M Hcl Solution In The Presence And Absence Of Dt At 303 K

Inhibitor	Concentration M $\times 10^{-4}$	R _p $\Omega \text{ cm}^2$	f _{max}	C _{dl}	$\eta\%$
Blank		16.89	7.55	1248	
DT	0.1	36.5	17.01	256	53.7
	5	38.3	17.13	243	56.4

Table 6. Quantum Chemical Parameters for D - Tryptophan (Dt)

Inhibitor	DT
E _{HOMO} (eV)	-5.064
E _{LUMO} (eV)	-1.287
ΔE (eV)	3.777
Absolute electronegativity (eV)	3.176
Global hardness (eV)	1.889
Global softness (eV)	0.529

Thus, the equivalent circuit depicted in Fig. 5 is employed to analyze the impedance spectra, where R_s represents the solution resistance, R_t denotes the charge-transfer resistance, and a CPE instead of a pure capacitor represents the interfacial capacitance. As seen from Table 5, the C_{dl} values decrease with the increase of DT concentration, which suggests that DT functions by adsorption on the mild steel surface. It is inferred that the DT molecules gradually replace the water molecules by adsorption at the metal/solution interface, which leads to the formation of a protective film on the mild steel surface and thus decreases the extent of the dissolution reaction [25]. Moreover, the increase of DT concentration leads to the increase of R_p and $\eta\%$ values.

Potentiodynamic polarization measurements

The anodic and cathodic potentiodynamic curves for mild steel in 2 M HCl solutions in the absence and presence of 1×10^{-5} M and 5×10^{-4} M of the DT at 30°C is shown in Fig. 3. The nature of the polarization curves remained the same in the absence and presence of the inhibitor, but the curves shifted towards lower current density in the presence of the inhibitor suggesting that the inhibitor molecules retard the corrosion process without changing the mechanism of the corrosion process. The polarization curves exhibit cathodic and anodic polarization curves with well defined Tafel regions. The electrochemical parameters such as corrosion potential (E_{corr}), corrosion current densities (i_{corr}), anodic Tafel slope (β_a), cathodic Tafel slope (β_b) and percentage inhibition efficiency ($\eta\%$) determined from the polarization curves are summarized in Table 4 with a maximum value for 5×10^{-4} M concentration of the inhibitors at 303 K as 78.4%. From table 4, it could be observed that the presence of different concentrations of DT molecules cause a decrease of the current density (i_{corr}) when the concentration of the DT is increased.

It is also observed that, the corrosion potential (E_{corr}) has no definite shift and the corrosion current densities (i_{corr}) decreases when the concentrations of the inhibitors increase indicating that the inhibitors adsorbed on the metal surface, and hence the inhibition efficiency increased with increasing inhibitor concentration causing small change in E_{corr} values implying that the inhibitors act as mixed type inhibitors affecting both the anodic and cathodic reactions. From the results, the changes of E_{corr} are less than 85mV, which indicate that DT acts as a mixed type inhibitor for the corrosion of MS in 2 M HCl solution.

Computational Calculations

The optimized geometry of DT is shown in Fig. 6 and their corresponding frontier molecular orbitals (HOMO and LUMO) are shown in Figs 7 and 8. The energy levels viz: E_{HOMO} , E_{LUMO} and ΔE calculated are depicted in Table 6. The energies of the frontier molecular orbital: E_{HOMO} and E_{LUMO} are significant parameters for the prediction of the reactivity of any chemical species. The frontier molecular theory describes that the formation of a transition state is due to an interaction between frontier molecular orbitals (HOMO and LUMO) of reacting species [28]. E_{HOMO} is associated with electron-donating ability of the inhibitor. As such, the inhibition efficiency of inhibitor is expected to increase with increasing value of E_{HOMO} since this indicates increasing ease of donating electrons to the vacant d-orbital of the metal. E_{LUMO} , on the other hand, is associated with the ability of the molecule to accept electron, therefore decreasing values of E_{LUMO} suggest better inhibition efficiency [29]. The energy gap of an inhibitor ($\Delta E = E_{LUMO} - E_{HOMO}$) is an important stability index and is used to develop theoretical models for explaining structure and conformation barriers in molecular systems. The smaller the energy gap, the better is the

expected inhibition efficiency of the compound [30]. According to the results in Table 6, the value of E_{HOMO} (-5.064eV) and the value of E_{LUMO} (-1.287eV) were found for D - Tryptophan (DT) affirming that D - Tryptophan (DT) has more potency to be adsorbed on the mild steel. The global hardness is the inverse of the global softness ($\eta = 1/S$). Values of S and η are presented in Table 6. The hard and soft acids as well as bases principle requires that a reaction between an acid and a base is favoured when global softness difference is minimal. Also, a hard molecule has a large energy gap while a soft molecule has a low energy gap.

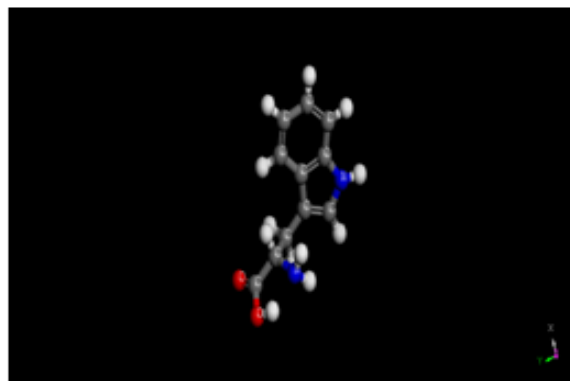


Fig 6. DFT-B3LYP Optimized Structure of D - TRYPTOPHAN (DT)

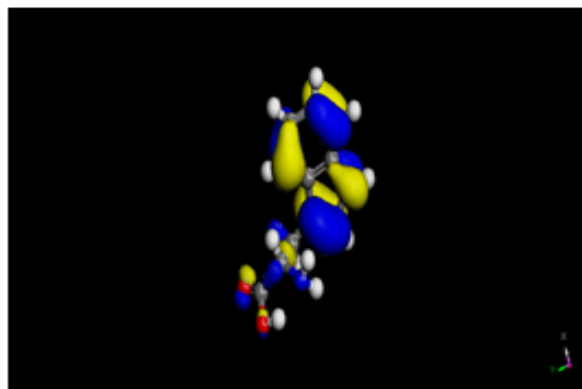


Fig 7. HOMO electronic density of D - TRYPTOPHAN (DT) molecule

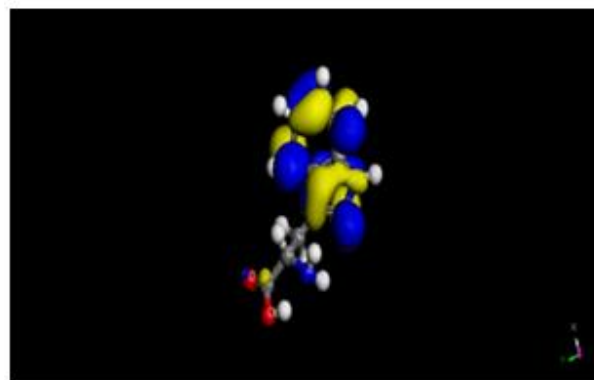


Fig 8. LUMO electronic density of D - TRYPTOPHAN (DT) molecule

Conclusions

The corrosion process was inhibited by adsorption of the D-tryptophan (DT) on the mild steel surface. The inhibition efficiency increases with increase in the concentration of DT but decreases with increase in temperature. Potentiodynamic polarization studies confirmed that the inhibitor acted through mixed type of corrosion inhibition mechanism. Computational

calculations show that apart from DT molecule adsorbing as cationic species on the mild steel surface, it can also adsorb as molecular species using oxygen, nitrogen and benzylic carbons as its active centres.

References

1. D. Gopi, K. M. Govindaraju, L. Kavitha, J. Appl. Electrochem. 40(2010) 1349 – 1356.
2. X. H. Li, G. N. Mu, Appl. Surf. Sci. 252 (2005) 1254 – 1265.
3. X. M. Li, L. B. Tang, L. LI, G. N. MU, G. H. Liu, Corros. Sci. 48 (2006) 308 – 321.
4. M. Lashkari, M. R. Arshadi, J. Chem. Phys. 299 (2004) 131.
5. N.O. Eddy, E.E. Ebenso, Int. J. Electrochem.Sci 5 (2010) 731.
6. I.B. Obot, N.O. Obi-Egbedi, Corros. Sci. 52 (2010) 198.
7. P.C. Okafor, E.E. Ebenso, U.J. Ekpe, Int. J. Electrochem.Sci 5 (2010) 978.
8. K. F. Khaled, Corrosion Science 50: (2010) 2905 – 2916
9. I.B. Obot, N.O. Obi-Egbedi, Corros. Sci. 52 (2010) 198.
10. N.O. Eddy, E.E. Ebenso, Int. J. Electrochem.Sci 5 (2010) 731.
11. P.C. Okafor, E.E. Ebenso, U.J. Ekpe, Int. J. Electrochem.Sci 5 (2010) 978.
12. I.B.Obot, N.O. Obi-Egbedi, S. A. Umoren, E. E. Ebenso, Int. J. Electrochem.Sci 5 (2010) 994.
13. E.E. Ebenso, H. Alemu, S.A. Umoren, I.B.Obot, Int. J. Electrochem. Sci. 3 (2008) 1325.
14. N. O. Obi-Egbedi, I. B. Obot, Arab. J. Chem. (2010). doi:10.1016/J.arabjch.2010.10.004.
15. H. Ashassi-Sorkhabi, B. Shaabani, and D. Seifzadeh, Applied surf. Sci. 239 (2005)154 - 164
16. A. Popova, E. Sokolova, S. Raicheva, M. Chritov, Corros. Sci. 45 (2003) 33 - 41
17. G. Quartarone, G. Moretti, A. Tassan, A. Zingale, Mater. Corros 45(1994) 641 - 647
18. M. Abdallah, E. A. Helal and A. S. Fouda, Corros. Sci. 48(2006)1639- 1645
19. Umoren, S. A., Obot, I. B., Ebenso, E. E. and Okafor, P. C. Portugaliae Electrochimica Acta 26 (2008) 267 - 287
20. F. Mansfeld, M. W. Kendig, S. Tsai, Corros. Sci. 38 (1982) 570 – 580.
21. S. Martinez, M. Metikos-Hukovic, J. Appl. Electrochem. 33 (2003) 1137 – 1142.
22. F. Bentiss, M. Lebrini, H. Vezin, F. Chai, M. Traisnel, M. Laggrenne, Corros. Sci. 51 (2009) 2165 – 2173.
23. J. L. Trinstancho-Reyes, M. Sanchez-Carrillo, R. Sandoval-Jabalera, V. M. Orozco-Carmona, F. Almeraya-Calderon, J. G. Chacon-Nava, J. G. Gonzalez-Rodriguez, A. Martinez-Villafarie, Int. J. Electrochem. Sci. 6 (2011) 419-431.
24. M. Kissi, M. Bouklah, B. Hammouti, M. Benkaddour, Appl. Surf. Sci. 252 (2006) 4190-4197.
25. F. Bentiss, M. Traisnel, M. Laggrenne, Corros. Sci. 42 (2000) 127 – 146.
26. M. Yadav , D. Behera, S. Kumur , R. R. Sinha, Industrial and engineering chemistry research 52 (2013) 6318 - 6328
27. M..Yadav, S. Kumar, D. Behera, Journal of Metallurgy 1 (2013) 1 - 15
28. K. Fukui, Springer-Verlag, New york, 1975.
29. G. Gokhan, Corros. Sci. 50 (2008), Pp. 2961 – 2992.
30. H. E. El Ashry, A. El Nemr, S. A. Esawy, and S. Ragab, Electrochim. Acta 51 (2006), Pp. 3957 – 3968.